Depleting Gene Activities in Early *Drosophila* Embryos with the "Maternal-Gal4–shRNA" System

Max V. Staller,* Dong Yan,† Sakara Randklev,†,‡ Meghan D. Bragdon,* Zeba B. Wunderlich,* Rong Tao,† Lizabeth A. Perkins,† Angela H. DePace,* and Norbert Perrimon†,‡,[1]

Departments of *Systems Biology and †Genetics and ‡Howard Hughes Medical Institute, Harvard Medical School, Boston, Massachusetts 02115

ABSTRACT In a developing *Drosophila melanogaster* embryo, mRNAs have a maternal origin, a zygotic origin, or both. During the maternal–zygotic transition, maternal products are degraded and gene expression comes under the control of the zygotic genome. To interrogate the function of mRNAs that are both maternally and zygotically expressed, it is common to examine the embryonic phenotypes derived from female germline mosaics. Recently, the development of RNAi vectors based on short hairpin RNAs (shRNAs) effective during oogenesis has provided an alternative to producing germline clones. Here, we evaluate the efficacies of: (1) maternally loaded shRNAs to knockdown zygotic transcripts and (2) maternally loaded Gal4 protein to drive zygotic shRNA expression. We show that, while Gal4-driven shRNAs in the female germline very effectively generate phenotypes for genes expressed maternally, maternally loaded shRNAs are not very effective at generating phenotypes for early zygotic genes. However, maternally loaded Gal4 protein is very efficient at generating phenotypes for zygotic genes expressed during mid-embryogenesis. We apply this powerful and simple method to unravel the embryonic functions of a number of pleiotropic genes.

DURING *Drosophila* oogenesis, the mother loads the oocyte with the RNAs and proteins necessary to support embryonic development until zygotic transcription begins ~2 hr after fertilization. Based on their expression patterns, three classes of genes can be distinguished: maternally expressed genes (referred to as "Mat"), zygotically expressed genes (referred to as "Zyg"), and genes expressed both maternally and zygotically (referred to as "Mat&Zyg") (for overview see Lawrence 1992). Characterization of the roles of Mat genes during embryonic development has classically been performed by examining the phenotypes of embryos laid by females carrying homozygous viable female sterile mutations. Examples of Mat genes include those that establish the anteroposterior [*bicoid* (*bcd*), *nanos* (*nos*), and *torso* (*tor*)] and dorsal–ventral [*dorsal* (*dl*)] axes (Lawrence 1992). Zyg genes have been identified among mutations associated with embryonic lethality, including those that interpret the maternally encoded positional information, such as gap [*e.g.*, *giant* (*gt*), *Kruppel* (*Kr*), and *knirps* (*kni*)], pair rule [*e.g.*, *fushi tarazu* (*ftz*), *even skipped* (*eve*), and *odd skipped* (*odd*)], and segment polarity [*e.g.*, *engrailed* (*en*), *wingless* (*wg*), and *hedgehog* (*hh*)] genes (see review by St. Johnston and Nusslein-Volhard 1992).

While many Mat and Zyg genes have been well characterized, the contributions of Mat&Zyg essential genes to embryonic development have yet to be fully described. Examining the null embryonic phenotypes of Mat&Zyg essential genes is technically challenging because embryos need to be derived from mutant germlines, *i.e.*, the functions cannot be examined from heterozygous mothers as the maternal contribution, in most cases, masks their early zygotic functions, and homozygous mutant females cannot be recovered as they are dead. A solution to this problem has been the creation of germline mosaics whereby eggs are collected from females with mutant homozygous germlines in an otherwise heterozygous soma. The most commonly used method to produce female germline mosaics is the *FLP-FRT ovoD* germline clone (GLC) technique (Chou and Perrimon 1996). Using this strategy, FLP-FRT–mediated mitotic recombination in an *ovoD* dominant female sterile background generates homozygous germline clones for

doi: 10.1534/genetics.112.144915
Manuscript received August 13, 2012; accepted for publication October 19, 2012
Supporting information is available online at http://www.genetics.org/lookup/suppl/doi:10.1534/genetics.112.144915/-/DC1.
[1]Corresponding author: Department of Genetics, Howard Hughes Medical Institute, Harvard Medical School, 77 Ave. Louis Pasteur, Boston, MA 02115. E-mail: perrimon@receptor.med.harvard.edu

candidate Mat&Zyg mutations in otherwise somatically heterozygous mutant females.

An example of a Mat&Zyg gene that yields diverse phenotypes when it is depleted at different stages of development is the *D-Raf* serine-threonine kinase (Perrimon *et al.* 1985; Ambrosio *et al.* 1989; see review by Duffy and Perrimon 1994). *D-raf* mutant offspring derived from heterozygous females die during larval–pupal development. However, embryos derived from *D-raf* mutant GLCs exhibit two classes of phenotypes: embryos that receive a WT paternal copy display a "terminal class" phenotype, with the acron and telson missing, because maternally derived D-raf gene product acts downstream of maternally derived Torso gene product, a receptor tyrosine kinase (RTK) that activates the Zyg genes *tailless* (*tll*) and *huckebein* (*hkb*). Embryos that do not receive a paternal copy show poor cuticle development, reflecting the role of D-raf downstream of another RTK, the epidermal growth factor receptor (EGFR), which is required for proper epidermal differentiation. While the EGFR phenotype can be paternally rescued, the terminal phenotype cannot, reflecting the early activity of Torso signaling and the later function of EGFR signaling. The *D-raf* example illustrates how different embryonic phenotypes can be observed depending on the level of either maternal or zygotic gene activity present at a specific developmental stage.

Recently, we established an alternative approach to GLCs based on RNA interference (RNAi). We generated vectors employing short hairpin RNAs (shRNAs) which, when expressed during oogenesis using an upstream activating sequence (UAS) and a maternal Gal4 driver, reproduced the phenotypes of Mat, Zyg, and Mat&Zyg genes (Ni *et al.* 2011). Using RNAi to study early embryonic phenotypes is an attractive strategy as it requires fewer and simpler crosses than the *FLP-FRT ovoD* method. Moreover, the easy production of *maternal-Gal4>>UAS-shRNA* females facilitates large-scale screening and the generation of large numbers of mutant embryos that can be used for phenotypic and biochemical analyses.

Extending the *maternal-Gal4>>UAS-shRNA* technique from oogenesis into early embryonic development is complicated by the maternal–zygotic transition (MZT), a period when maternal mRNAs are degraded and gene expression comes under the control of the zygotic genome (Tadros and Lipshitz 2009). This constraint led us to evaluate in detail the use of the Gal4-UAS system to drive shRNA expression in early embryos. Specifically, we determined whether maternal loading of shRNAs into embryos could deplete zygotic RNAs and to what extent maternally provided Gal4 could be used to express zygotic shRNAs at sufficient levels to generate mutant phenotypes (Figure 1). Our results indicate that while Gal4-driven shRNAs in the female germline targeting maternal transcripts are extremely effective at generating phenotypes consistent with strong knockdown, maternally loaded shRNAs targeting zygotic transcripts are not very effective at yielding phenotypes. However, maternally loaded

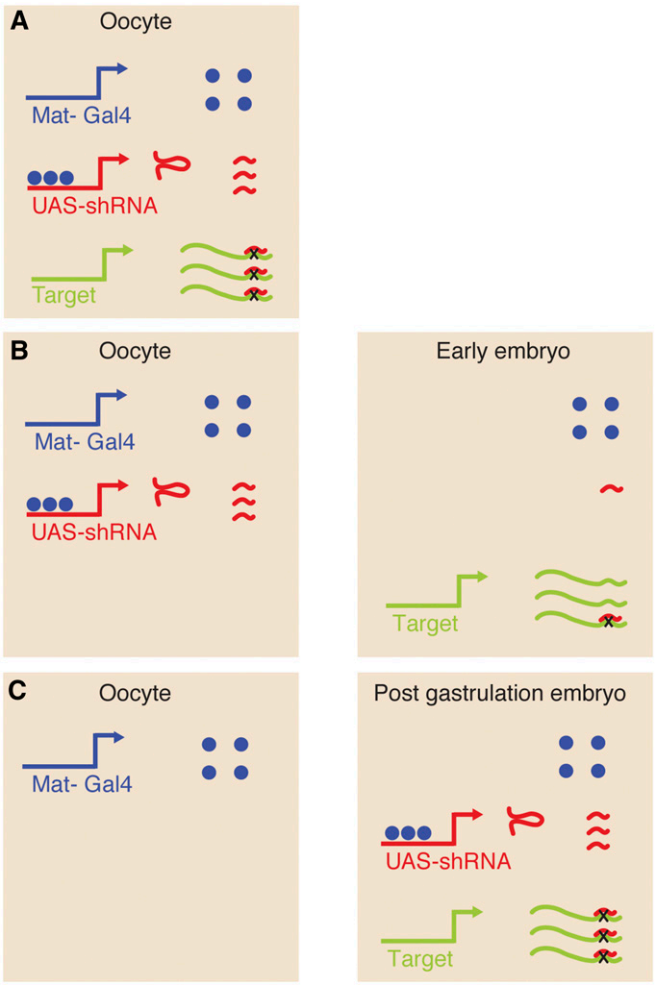

Figure 1 Strategies for knockdown of maternal and zygotic transcripts. (A) Depletion of a maternal transcript following expression of shRNAs in the female germline. The maternal Gal4 driver (blue) activates shRNAs (red), which deplete target transcripts (green). (B) Depletion of a zygotic transcript by loading the embryo with maternally derived shRNAs. (C) Depletion of a zygotic transcript following zygotic activation of shRNAs by maternally loaded Gal4 protein. Strategies A and B correspond to F_2 phenotypes in Table 1 while strategy C corresponds to an F_1 phenotype.

Gal4 protein is very efficient at activating zygotic *UAS-shRNA* constructs and generating phenotypes for genes expressed during mid-embryogenesis. We illustrate these features of the "maternal-Gal4–shRNA" system and apply the method to the identification of a number of new zygotic lethal loci with specific maternal effect phenotypes.

Materials and Methods

Drosophila strains

Two different maternal Gal4 drivers (*maternal-Gal4*) were used: (1) Maternal triple driver Gal4 (*MTD-Gal4*): *(P(otu-Gal4::VP16.R)1, w[*]; P(Gal4-nos.NGT)40; P(Gal4::VP16-nos.UTR)CG6325[MVD1])*, described in Petrella *et al.* (2007) (Bloomington Stock no. 31777), a gift from L. Cooley. These

flies are homozygous for three Gal4 transgenes that together drive expression through all of oogenesis. *P(otu-Gal4::VP16.R)* contains the *ovarian tumor* (*otu*) promoter and *fs(1)K10* 3′-untranslated region (UTR) and drives strong expression beginning in stage 1 egg chambers. *P(Gal4-nos.NGT)* contains the *nos* promoter and 3′-UTR, driving expression throughout the germarium. *P(Gal4::VP16-nos.UTR)* contains the *nos* promoter and *αTubulin84E* 3′-UTR and drives expression through oogenesis. (2) Maternal-tubulin-Gal4 (*mat-tub-Gal4*) driver: *y w*; *P(mat-tub-Gal4)mat67*; *P(mat-tub-Gal4)mat15* (line 2318) is from D. St. Johnston and F. Wirtz-Peitz. This line is homozygous for two insertions of a construct containing the maternal tubulin promoter from *αTub67C* and the 3′-UTR from *αTub84B*. The difference between *MTD-Gal4* and *mat-tub-Gal4* driver lines is that *mat-tub-Gal4* does not drive expression during early oogenesis in the germarium. This difference is useful, as in some cases early oogenesis defects that can be detected with *MTD-Gal4* can be bypassed using *mat-tub-Gal4*, thus allowing the production of eggs (D. Yan and N. Perrimon, unpublished data). Timing aside, the two drivers led to similar embryonic phenotypes and were used interchangeably in this study. Finally, all mutant alleles were obtained from the Bloomington *Drosophila* Stock Center: *hb[12]* (no. 1755), *kni[1]* (no. 1783), *Kr[2]* (no. 1601), *eve[1]* (no. 1599), *hkb[2]* (no. 5457), *twi[1]* (no. 2381), *fkh[6]* (no. 545), *en[7]* (no. 1820), *ftz[11]* (no. 1841), *hh[21]* (no. 5338), *sna[1]* (no. 25127), and *wg[l-17]* (no. 2980).

The two UAS-shRNA vectors used in this screen are described in Ni *et al.* (2011). VALIUM20 is effective in both the soma and female germline, and VALIUM22 is more potent in the female germline and less efficient in the soma. The constructs used in this study were generated at the Transgenic RNAi Project (TRiP) at Harvard Medical School and integrated into the genome at either the attP2 (chromosome III) or attP40 (chromosome II) landing sites, as previously described (Ni *et al.* 2011). Details on the lines used in this study can be found in Table 1 and on the TRiP website (http://www.flyrnai.org).

Testing for embryonic phenotypes

To determine F_1 phenotypes, ~10 *maternal-GAL4* females were crossed with ~5 *UAS-shRNA* homozygous or heterozygous males and embryos collected at 27°. For the F_2 phenotype analyses, *maternal-GAL4>>UAS-shRNA* females were recovered from the previous cross and mated to either their siblings or *UAS-shRNA* homozygous males. In the few cases where F_1 crosses failed to give progeny (see Table 1), *maternal-GAL4>>UAS-shRNA* flies were generated by crossing *maternal-GAL4* males with *UAS-shRNA* females. Note that all crosses were performed at 27° as Gal4 is more potent at higher temperatures. We avoided testing the flies at 29° because of some male sterility issues at this temperature.

The percentage of embryos hatching was determined by lining up approximately two hundred 0- to 24-hr embryos and counting the dead (brown) and hatched eggs after at least 24 hr. When lethality was observed, cuticles were prepared to examine patterning defects. Unhatched cuticles were prepared and mounted in Hoyer's mounting media. For images in Figure 4, a *Z*-stack of 3–6 images was acquired and computationally flattened using Helicon Focus software (HeliconSoft).

Design of new scaffold shRNA vectors

A number of stable maternally deposited mRNAs have been identified by Votruba (2009). Hairpin pre-miRNA sequences for miR-275 and miR-92a were downloaded from miRbase (Kozomara and Griffiths-Jones 2011). The shRNAs were inserted into the 21 bp that normally become the mature miRNA, and the complementary portion of the hairpin made into a perfect match. All oligos used are listed in supporting information, Table S1. Note that all of the pre-miRNA hairpin sequence is included in the oligos and that no other changes were made to the VALIUM20 backbone. Complementary oligos were annealed and cloned into the *Nhe*I and *Eco*RI sites of VALIUM20 and injected into the attP2 landing site. Injections were performed by Genetic Services, Inc. (GSI) (http://www.geneticservices.com).

In situ hybridization

Embryos from *MTD-GAL4>>UAS-shRNA-hb* mothers were collected for 8 hr, fixed in heptane and formaldehyde for 25 min, stained with dinitrophenol (DNP) probes against *hb*, and fluorescently detected by horseradish peroxidase/tyramide deposition of Cy3 (Perkin Elmer) as described in Fowlkes *et al.* (2011). Images were acquired by laser scanning microscopy with two-photon excitation at 750 nm (Luengo Hendriks *et al.* 2006). Briefly, the sytox green nuclear stain was used to automatically identify nuclei and the Cy3 signal in each nucleus was quantified (Luengo Hendriks *et al.* 2006). Analysis of expression domain boundaries was performed in MatLab (Mathworks) using the PointCloud toolbox from the Berkeley *Drosophila* Transcription Network Project (BDTNP, http://bdtnp.lbl.gov/Fly-Net/). Embryo length was normalized and expression boundaries were detected by finding the inflection point in the pattern. WT data were downloaded from http://bdtnp.lbl.gov/Fly-Net/ (Fowlkes *et al.* 2008).

Results and Discussion

shRNAs expressed in the female germline effectively knock down Mat genes

To extend our previous finding that shRNAs expressed during oogenesis effectively knockdown maternally deposited transcripts, we tested a number of UAS-shRNA lines targeting various Mat genes. shRNA lines were produced against *bcd*, *tor*, *nos*, and *dl*, and all exhibited embryonic phenotypes commensurate with strong mutant alleles (Table 1, Figure 2). These data suggest that shRNAs driven by mat-GAL4 are very effective at depleting the relevant transcripts in the female germline.

Table 1 Phenotypic analysis of shRNA lines

Line	Gene name	Vector	Gal4 line	F_1 phenotype	F_2 phenotype
Mat genes					
HMS00930	nanos (nos)	VALIUM20	mat-tub-Gal4	No	100%, nanos
GL00407	bicoid (bcd)	VALIUM22	mat-tub-Gal4	No	100%, bicoid
GL01320	bicoid (bcd)	VALIUM22	MTD-Gal4	No	100%, bicoid
HMS00727	dorsal (dl)	VALIUM20	mat-tub-Gal4	No	100%, dorsalized
GL00610	dorsal (dl)	VALIUM22	mat-tub-Gal4	No	100%, dorsalized
GL00222	torso (tor)	VALIUM22	mat-tub-Gal4	No	80%, weak torso
HMS00021	torso (tor)	VALIUM20	mat-tub-Gal4	No	100%, torso
Zyg genes					
HMS00595	engrailed (en)	VALIUM20	mat-tub-Gal4	No	No
HMS01312	even skipped (eve)	VALIUM20	mat-tub-Gal4	No	No
HMS01105	giant (gt)	VALIUM20	mat-tub-Gal4	No	No
GL01317	giant (gt)	VALIUM22	MTD-Gal4	No	No
GL01318	giant (gt)	VALIUM22	MTD-Gal4	No	No
GL01319	giant (gt)	VALIUM22	mat-tub-Gal4	No	No
HMS00492	hedgehog (hh)	VALIUM20	mat-tub-Gal4	No	No
HMS01216	huckebein (hkb)	VALIUM20	mat-tub-Gal4	No	No
HMS01184	knirps (kni)	VALIUM20	mat-tub-Gal4	No	No
HMS01106	Kruppel (Kr)	VALIUM20	mat-tub-Gal4	No	No
GL01322	Kruppel (Kr)	VALIUM22	MTD-Gal4	No	No
GL01323	Kruppel (Kr)	VALIUM22	mat-tub-Gal4	No	No
GL01324	Kruppel (Kr)	VALIUM22	MTD-Gal4	No	No
HMS01186	runt (run)	VALIUM20	mat-tub-Gal4	No	No
HMS01108	sloppy paired 2 (slp2)	VALIUM20	mat-tub-Gal4	No	No
HMS01313	hairy (h)	VALIUM20	mat-tub-Gal4	No	No
HMS01317	twist (twi)	VALIUM20	mat-tub-Gal4	No	No
HMS01215	brother of odd with entrails limited (bowl)	VALIUM22	mat-tub-Gal4	No	No
HMS01122	crocodile (croc)	VALIUM20	mat-tub-Gal4	No	No
HMS01150	Dichaete (D)	VALIUM20	mat-tub-Gal4	No	No
HMS01103	forkhead (fkh)	VALIUM20	mat-tub-Gal4	No	No
HMS01104	fushi tarazu (ftz)	VALIUM20	mat-tub-Gal4	No	No
HMS01552	knirps like (knl)	VALIUM20	mat-tub-Gal4	No	No
HMS01315	odd-skipped (odd)	VALIUM20	mat-tub-Gal4	No	No
HMS01314	orthodenticle (otd)	VALIUM20	mat-tub-Gal4	No	No
HMS01167	schnurri (schn)	VALIUM20	mat-tub-Gal4	No	No
HMS01107	sloppy paired 1 (slp1)	VALIUM20	mat-tub-Gal4	No	No
HMS01252	snail (sna)	VALIUM20	mat-tub-Gal4	No	No
HMS00794	wingless (wg)	VALIUM20	mat-tub-Gal4	No	No
HMS00844	wingless (wg)	VALIUM20	mat-tub-Gal4	No	No
HMS01109	zerknult 1 (zen1)	VALIUM20	mat-tub-Gal4	No	No
HMS01124	zerknult 2 (zen2)	VALIUM20	mat-tub-Gal4	No	No
HMS00545	outstretched (os)	VALIUM20	mat-tub-Gal4	No	No
HMS01316	tailless (tll)	VALIUM20	mat-tub-Gal4	No	No
HMS00922	paired (prd)	VALIUM20	mat-tub-Gal4	No	No
HMS01443	teashirt (tsh)	VALIUM20	mat-tub-Gal4	No	No
JF02455	decapentaplegic (dpp)	VALIUM20	mat-tub-Gal4	60%, retraction defects	100%, ventralized
Mat&Zyg genes					
HMS01414	armadillo (arm)	VALIUM20	mat-tub-Gal4	100%, segment polarity	NT
HMS01414	armadillo (arm) (reverse cross)	VALIUM20	mat-tub-Gal4	No	100%, segment polarity
HMS00009	Notch (N)	VALIUM20	mat-tub-Gal4	95%, neurogenic embryos	NT
HMS00009	Notch (N) (reverse cross)	VALIUM20	mat-tub-Gal4	No	NT
GL00092	Notch (N)	VALIUM22	mat-tub-Gal4	10%, neurogenic embryos	75%, neurogenic
HMS00647	domeless (dome)	VALIUM20	mat-tub-Gal4	No	90%, JAK/STAT variable
HMS01293	domeless (dome)	VALIUM20	mat-tub-Gal4	100%, head defects	NT
HMS00856	rhea	VALIUM20	mat-tub-Gal4	100%, cuticles WT	NT
HMS00799	rhea	VALIUM20	mat-tub-Gal4	100%, cuticles WT	100%, dorsal cuticle defects
HMS00239	canoe (cno)	VALIUM20	mat-tub-Gal4	No	100%, dorsal open
GL00633	canoe (cno)	VALIUM22	mat-tub-Gal4	No	100%, dorsal open
GL01321	hunchback (hb)	VALIUM22	mat-tub-Gal4	No	90% head defect, some segmentation defects

(continued)

Table 1, *continued*

Line	Gene name	Vector	Gal4 line	F_1 phenotype	F_2 phenotype
HMS00743	upheld (up)	VALIUM20	mat-tub-Gal4	100%, head defects, segments compressed	NT
HMS00076	Helicase at 25E (Hel25E)	VALIUM20	mat-tub-Gal4	Many dead embryo with WT cuticle/dead L1 dead/few adults	100%, abnormal oogenesis
HMS00187	Proteasome beta3 subunit (Prosbeta3)	VALIUM20	mat-tub-Gal4	Some brown eggs, mostly larvae lethal, very few adults	NT
HMS00526	Not1	VALIUM20	mat-tub-Gal4	Larval lethal, very few adults	NT
HMS00043	myospheroid (mys)	VALIUM20	mat-tub-Gal4	85%, variable cuticles, few larvae, few adults	NT
HMS00310	pasilla (pas)	VALIUM20	mat-tub-Gal4	85%, cuticles WT, few larvae, very few adults	NT
HMS01417	tumbleweed (tum)	VALIUM20	mat-tub-Gal4	80%, cuticles WT, few larvae, very few adults	NT
HMS00274	small nuclear ribonucleoprotein 70K (snrp70K)	VALIUM20	mat-tub-Gal4	80%, variable, few larvae, very few adults	NT
HMS00693	shotgun (shg)	VALIUM20	mat-tub-Gal4	80%, some dorsal closure defects, few larvae, few adults	NT
HMS00580	trithorax (trx)	VALIUM20	mat-tub-Gal4	Few dead embryos, cuticle WT, larval lethality, few adults	NT
HMS01009	Sirt6	VALIUM20	mat-tub-Gal4	80%, cuticles WT, few larvae, no adults	NT
HMS00968	Ribosomal protein S15Aa (Rps15Aa)	VALIUM20	mat-tub-Gal4	80%, cuticles WT, few larvae, very few adults	NT
HMS00084	cactus (cac)	VALIUM20	mat-tub-Gal4	No	100%, ventralized
GL00627	cactus (cac)	VALIUM22	mat-tub-Gal4	No	100%, ventralized
HMS00317	α Catenin (a-Cat)	VALIUM20	mat-tub-Gal4	No	99%, blobbed or segment polarity
HMS01662	PDGF- and VEGF-receptor related (Pvr)	VALIUM20	mat-tub-Gal4	No	100%, of embryos unhatched, WT cuticle
HMS00276	split ends (spen)	VALIUM20	mat-tub-Gal4	No	99%, of embryos with U-shaped and head defects
HMS00105	gawky (gw)	VALIUM20	mat-tub-Gal4	No	100%, abnormal oogenesis, fused filaments, a few brown eggs
HMS00079	glorund (glo)	VALIUM20	mat-tub-Gal4	No	95%, some JAK/STAT
HMS00352	RhoGAP19D	VALIUM20	mat-tub-Gal4	No	50% embryos anterior holes
HMS00810	capulet (capt)	VALIUM20	mat-tub-Gal4	No	99%, some U-shaped
HMS00318	Chromosome-associated protein (Cap)	VALIUM20	mat-tub-Gal4	No	100%, mostly blobbed
GL00047	Autophagy-specific gene 1 (Atg1)	VALIUM22	mat-tub-Gal4	No	80%, some head defects
HMS00256	Mediator complex subunit 25 (Med 25)	VALIUM20	mat-tub-Gal4	No	95%, some blobbed, some U-shaped
HMS00012	corkscrew (csw)	VALIUM20	mat-tub-Gal4	No	100%, weak corkscrew
HMS01618	zipper (zip)	VALIUM20	mat-tub-Gal4	No	100%, abnormal oogenesis, few abnormal eggs
HMS00035	Signal-transducer and activator of transcription protein at 92E (Stat92E)	VALIUM20	mat-tub-Gal4	No	100%, JAK/STAT phenotype
HMS00238	connector enhancer of ksr (cnk)	VALIUM20	mat-tub-Gal4	No	80%, weak terminal class
HMS00087	Histone deacetylase 3 (Hdac3)	VALIUM20	mat-tub-Gal4	100%, head defects	100%, ventralized
HMS00149	Son of sevenless (sos)	VALIUM20	mat-tub-Gal4	No	100%, weak terminal class
JF02287	discs large 1 (dlg1)	VALIUM20	mat-tub-Gal4	No	100%, blobbed and dorsal open

(continued)

Table 1, *continued*

Line	Gene name	Vector	Gal4 line	F_1 phenotype	F_2 phenotype
HMS00111	archipelago (ago)	VALIUM20	mat-tub-Gal4	No	50%, pair rule phenotype
HMS00284	Ubiquitin-63E (Ubi-63E)	VALIUM20	mat-tub-Gal4	No	100%, No development
HMS00052	cap binding protein 80 (cpb80)	VALIUM20	mat-tub-Gal4	100% cuticles WT	No eggs
HMS00128	Elongin C	VALIUM20	mat-tub-Gal4	No	100%, white eggs
HMS00802	lethal (2) NC136 (l(2)NC136)	VALIUM20	mat-tub-Gal4	100% cuticles WT	No eggs
HMS00145	Downstream of raf1 (Dsor1)	VALIUM20	mat-tub-Gal4	No	100%, terminal defects
HMS00173	rolled (rl)	VALIUM20	mat-tub-Gal4	No	100%, blobbed, terminal defects
GL00215	rolled (rl)	VALIUM22	MTD-Gal4	No	100%, blobbed, terminal defects
HMS02519	Kruppel (Kr)	VALIUM20-miR92a	mat-tub-Gal4	WT	WT
HMS02518	Notch (N)	VALIUM20-miR92a	mat-tub-Gal4	Neurogenic	100% neurogenic
HMS02520	armadillo (arm)	VALIUM20-miR92a	mat-tub-Gal4	Segment polarity	NT
HMS02521	bicoid (bcd)	VALIUM20-miR92a	mat-tub-Gal4	NT	100%, bicoid
HMS02522	wingless (wg)	VALIUM20-miR92a	mat-tub-Gal4	WT	WT
HMS02516	giant (gt)	VALIUM20-miR275	mat-tub-Gal4	NT	WT
HMS02517	ovarian tumor (otu)	VALIUM20-miR275	mat-tub-Gal4	NT	Few eggs
HMS02511	bicoid (bcd)	VALIUM20-miR275	mat-tub-Gal4	NT	100%, bicoid

Unless indicated as "reverse cross" maternal-Gal4 females were crossed to shRNA males. F_1 *maternal-Gal4>>UAS-shRNA* females were crossed to sibling males heterozygous for the *UAS-shRNAs*. %, the fraction of unhatched eggs; no, embryos have normal viability; NT, not tested.

Maternally loaded shRNAs are not very effective at knocking down early acting Zyg genes

Next, we tested whether maternal loading of shRNAs was efficient at knocking down Zyg genes. We generated UAS-shRNA lines against 30 of the earliest known zygotic genes that are not expressed during oogenesis (Table 1). Embryos derived from *maternal-Gal4>>UAS-shRNAs* females crossed to sibling males heterozygous for *UAS-shRNA* were examined for embryonic phenotypes. Strikingly, only the shRNA line that targeted *decapentaplegic* (*dpp*) showed embryonic lethality, with 100% of the F_2 embryos exhibiting a ventralized phenotype (Table 1, *dpp*-F_2 phenotype in Figure 2). Although we cannot be certain that all the UAS-shRNA lines are effective at knocking down the targeted transcripts, these results indicate that most shRNAs delivered from the mother to the embryo do not sufficiently deplete early zygotic transcripts to generate embryonic phenotypes detectable in the cuticle. Regardless, the phenotype for zygotic *dpp* transcripts with maternal shRNAs indicates that maternally derived shRNAs can work [see also below results from *hunchback* (*hb*)].

Our ability to detect a cuticle phenotype for *dpp* most likely reflects the haploinsufficiency associated with this gene (Spencer *et al.* 1982) that renders it more sensitive to knockdown. Importantly, depletion of *dpp* suggested the possibility that some of our shRNA constructs were ineffective not because the hairpin did not work, but because an insufficient amount of maternally derived shRNA was present in early embryos. Thus, we tested whether reducing by half the amount of zygotic gene product in embryos derived from *maternal-Gal4>>UAS-shRNA* females could reveal phenotypes. Crossing *maternal-Gal4>>UAS-shRNA* females to mutant heterozygous males created embryos with the same amount of maternally deposited shRNA but (presumably) half the number of zygotic transcripts for the targeted gene. We looked for phenotypes in sensitized backgrounds for the following genes: *Kr*, *kni*, (gap); *hkb*, *fork head* (*fkh*) (terminal); *eve*, *ftz* (pair rule); *twist* (*twi*), *snail* (*sna*) (dorsal–ventral); *wg*, *hh*, and *en* (segment polarity), and were able to detect clear phenotypes for shRNAs targeting *Kr* and *twi*. In the case of *twi*, ~50% of the embryos showed the expected twisted phenotype (Figure 2). For *Kr*, 25% of the embryos showed a mild gap segmentation phenotype detectable by the absence of the second abdominal segment (A2) (Figure 2). Similarly, for *ftz* we observed ~30% lethality and a mild phenotype where one thoracic segment was missing. In addition, for the segment polarity genes *hh* and *wg*, we found rare embryos with cuticle defects similar to those of classic mutant alleles (Figure 2). Altogether, these results indicate that maternally loaded shRNAs targeting early zygotically expressed genes are more efficient in a sensitized heterozygous mutant background.

New shRNA backbones for depletion of early zygotic transcripts

The shRNA sequences in VALIUM20 are embedded in the *miR-1* backbone that is not expressed during oogenesis and early embryogenesis (Ruby *et al.* 2007). To test whether shRNAs would be more effective when expressed in the backbone of a miRNA normally expressed during late oogenesis and embryogenesis, we generated transgenic lines targeting the *otu*, *Notch* (*N*), *bcd*, *Kr*, *gt*, *wg*, and *armadillo* (*arm*) genes in the backbone of *miR-275* and *miR-92a*, as both had been shown previously to be some of the most stable miRNAs present in unfertilized embryos (Votruba

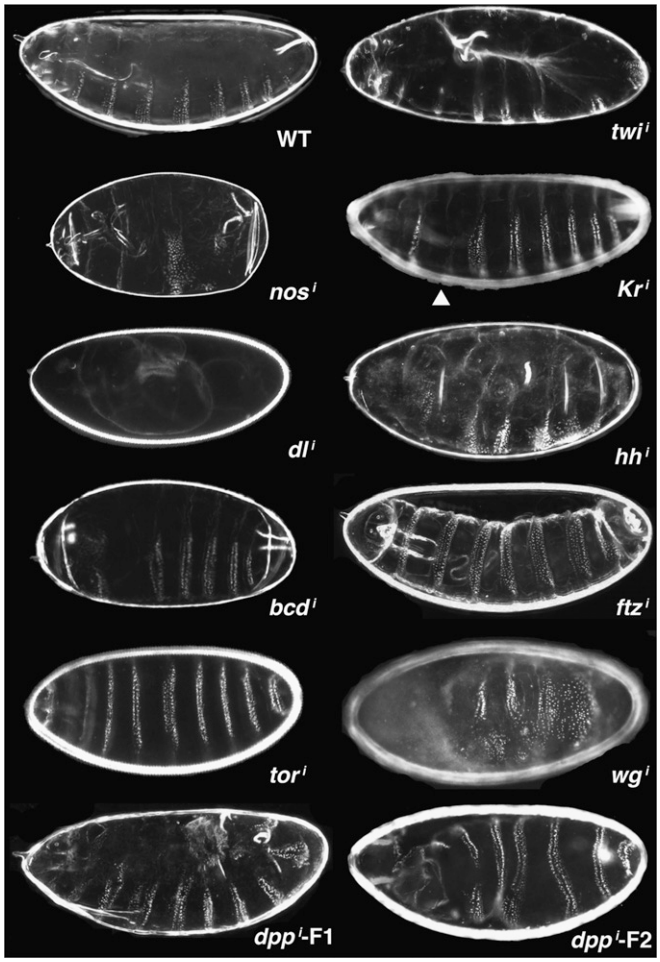

Figure 2 Embryonic phenotypes associated with knockdown of Mat and Zyg genes. For *nos*, *dl*, *bcd*, *tor*, and *dpp-F2*, *mat-tub-Gal4>>UAS-shRNA* mothers were crossed to *UAS-shRNA* males. All phenotypes resemble strong classic alleles. *dpp-F1* embryos were obtained from crossing *mat-tub-Gal4* females to *UAS-shRNA* males. For *Kr*, *twi*, *hh*, *ftz*, *and wg*, *mat-tub-Gal4>>UAS-shRNA* mothers were crossed to males heterozygous for a strong mutant allele of the target gene. Only a subset (see text) of embryos from these crosses had cuticle phenotypes. The phenotypes for *twi*, *hh*, and *wg* resemble classic mutants. For *Kr*, the main defect is the absence of the A2 segment (arrowhead), which is a smaller gap than seen in classic mutant embryos. The same phenotype was observed with two shRNA lines (GL01322 and GL01324). For *ftz*, the embryos are missing two anterior segments, a weaker phenotype than is seen in classic mutant embryos. Description of the mutant phenotypes and references for each gene tested can be found at http://flybase.org/. WT refers to a wild-type cuticle. The "i" superscript refers to the RNAi-induced phenotypes.

2009). Although shRNAs targeting *bcd*, *otu*, *N*, and *arm* generated phenotypes comparable to the original lines in the *miR-1* design (Table 1), shRNAs against *Kr*, *gt*, and *wg* did not. Thus, backbones of miRNAs expressed or not during oogenesis do not appear to make a significant difference. Further studies that quantify the respective amounts of shRNAs produced with the various designs and that determine the stability of the shRNAs will be needed to evaluate whether the system can be improved further.

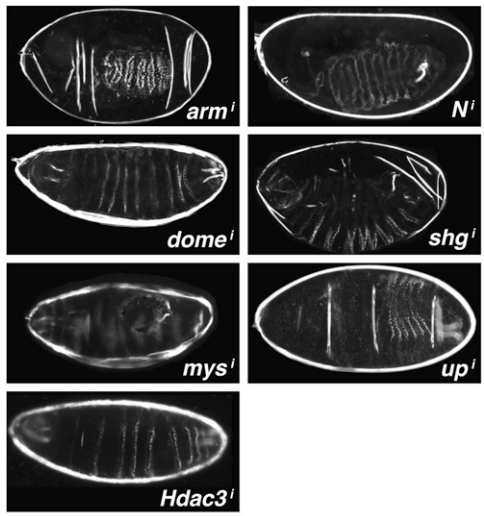

Figure 3 Zygotic phenotypes revealed by the expression of zygotic shRNAs by maternally loaded Gal4 protein. For some genes, high rates of F_1 lethality and specific embryonic phenotypes were detected when *maternal-Gal4* females were crossed to *UAS-shRNA* males. These included *armadillo* (*arm*), *Notch* (*N*), *domeless* (*dome*), *shotgun* (*shg*), *myospheroid* (*mys*), *upheld* (*up*), and *Histone deacetylase 3* (*Hdac3*). Additional shRNA lines associated with F_1 phenotypes are listed in Table 1.

Maternally loaded Gal4 protein can trigger zygotic expression of shRNAs

To our surprise, maternally deposited Gal4 protein can activate zygotic expression of *UAS-shRNA* transgenes early enough and strongly enough to generate cuticle phenotypes. We observed significant F_1 lethality (60%) in embryos derived from crossing *mat-tub-Gal4* females with *UAS-shRNA-dpp* homozygous males (*dpp*-F_1 phenotype in Figure 2). These embryos showed variable germ band retraction and head defect phenotypes reminiscent of weak *dpp* alleles, (Spencer *et al.* 1982; Irish and Gelbart 1987). In addition, a number of shRNAs targeting other genes also led to F_1 embryonic lethality and in some cases cuticle phenotypes (see "F_1 phenotype" column in Table 1, Figure 3). Two striking examples are *arm* (the *Drosophila melanogaster* β-catenin homolog) and *N*. All embryos derived from *mat-tub-Gal4* females crossed to *UAS-shRNA-arm*, but not from the reciprocal cross, showed the stereotypical segment polarity phenotype reflecting the role of β-catenin in Wg signaling (Peifer *et al.* 1991) (Figure 3). Similarly, most F_1 embryos (95%) from *mat-tub-Gal4* females crossed to *UAS-shRNA-N* (line HMS0009), but not from the reverse cross, showed a neurogenic phenotype (Figure 3). Note that the VALIUM22 line against *N* (GL00092) showed lower F_1 lethality (10%), most likely reflecting the difference between the VALIUM20 and VALIUM22 expression vectors (Ni *et al.* 2011; *Materials and Methods*). Interestingly, crossing *mat-tub-Gal4>>UAS-shRNA-N* females to sibling males resulted in 75% neurogenic embryos, with the remaining quarter of the progeny surviving. This fraction is consistent with the

quarter of embryos without a *UAS-shRNA-N* transgene surviving and reminiscent of the previously reported paternal rescue of the Notch maternal effect phenotype (Lehmann *et al.* 1981). Together, these data suggest how, for genes expressed after gastrulation, maternal Gal4 can activate zygotically delivered shRNAs to strongly deplete target transcripts.

Varying UAS-shRNA copy number to reveal different discrete phenotypes

The ability of maternal Gal4 to activate shRNAs in both the germline and the zygote has implications for detecting and interpreting embryonic phenotypes associated with the knockdown of Mat&Zyg genes. An instructive example is the case of *rolled* (*rl*), the *Drosophila* MAPK/ERK serine/threonine kinase that acts downstream of RTKs such as Tor and EGFR. Previous studies have shown that these RTKs activate a sequential signaling cascade of the D-Raf, D-MEK, and MAPK/Rl kinases (Duffy and Perrimon 1994; Li 2005). However, while the roles of D-Raf and D-MEK in Tor signaling have been well characterized by the analysis of their GLC phenotypes (Duffy and Perrimon 1994; Li 2005), Rl has only been implicated in Tor signaling by the ability of a *rl* loss-of-function mutation to suppress a gain-of-function Tor mutation (Brunner *et al.* 1994). Strikingly, different classes of embryonic cuticles are observed, depending on the genotypes of the males that are crossed to *MTD-Gal4>>UAS-shRNA-rl* females. If we crossed *MTD-Gal4>>UAS-shRNA-rl* females to WT males, 50% of the embryos showed terminal defects (the torso "terminal class" phenotype) (Figure 4A1), while the other half showed poor cuticle development (the EGFR mutant phenotype) (Figure 4A2). On the other hand, 100% of the embryos derived from *MTD-Gal4>>UAS-shRNA-rl* females crossed to *UAS-shRNA-rl* homozygous males showed poor cuticle development, similar to those shown in Figure 4A2. These distributions indicate that the presence of zygotic *UAS-shRNA-rl* influences the phenotype of embryos derived from *MTD-Gal4>>UAS-shRNA-rl* females. Embryos with either one or two copies of the *UAS-shRNA-rl* transgene show poor cuticle development, reflecting a role of Rl in EGFR signaling. In contrast, paternally rescued embryos without a *UAS-shRNA* transgene develop a terminal class phenotype consistent with Rl acting downstream of Tor. Altogether, these results are reminiscent of the phenotypes observed from *D-raf* GLCs (see Introduction) and demonstrate that the presence of the shRNA transgene in the embryo needs to be carefully followed to interpret the mutant phenotypes. Importantly, when *MTD-Gal4>>UAS-shRNA* females are crossed to *UAS-shRNA* males, some embryos will carry two and others a single *UAS-shRNA* transgene, which may also account for differences in the severity of embryonic phenotypes. Thus, varying the copy number of zygotic *UAS-shRNA* transgenes provides a useful way to generate phenotypic series and uncover when pleiotropic genes are used in development.

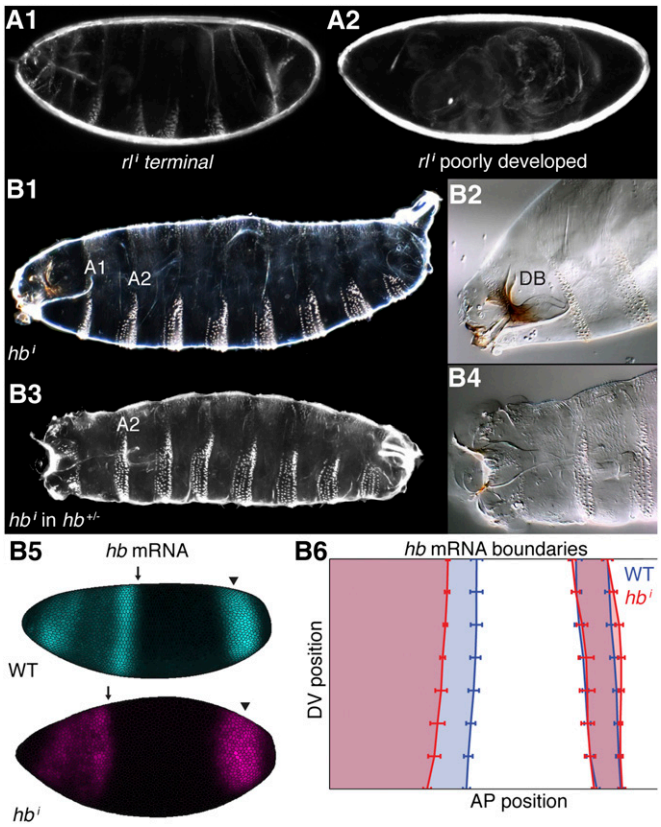

Figure 4 Embryonic phenotypes associated with *rolled* and *hunchback* shRNAs. (A) *rolled*. When *MTD-Gal4>>UAS-shRNA-rl* (*GL215*) females were crossed to WT males, the embryos showed differentiated cuticles with terminal defects (A1). However, when crossed to *UAS-shRNA-rl* homozygous males, all embryos show poor cuticle development (A2). These phenotypes reflect the role of Rl/MAPK in the Tor and EGFR RTK pathways, respectively (see text). (B) *hunchback*. Embryos from *MTD-Gal4>>UAS-shRNA-hb* mothers crossed to WT fathers are missing the T2 and T3 thoracic segments, while abdominal segmentation is normal (B1). B2 shows the head of embryo in B1. Note that the dorsal bridge (DB) is present and appears normal. When we crossed *MTD-Gal4>>UAS-shRNA-hb* females to WT males, we could not distinguish between embryos with zero or one copy of the *UAS-shRNA-hb* transgene. Similarly, when we crossed *MTD-Gal4>>UAS-shRNA-hb* females to *UAS-shRNA-hb* homozygous males, we could not distinguish between embryos with one or two copies of the *UAS-shRNA-hb* transgene; all three classes of embryos resembled the one shown in B1 and B2. Together these results demonstrate that zygotically expressed shRNAs do not contribute meaningfully to this phenotype. However, when *MTD-Gal4>>UAS-shRNA-hb* mothers were crossed to *hb[12]*/+ males, half of the embryos showed a more severe phenotype (B3). In addition to lacking T2 and T3, these embryos lack the A1 abdominal segment and head structures (B4). Computational representation of *hb* mRNA (maternal and zygotic) *in situ* hybridizations in mid blastoderm stage embryos. The arrow indicates the shift in the anterior expression domain, and the arrowhead indicates that the posterior pattern has not shifted (B5). mRNA expression domain boundaries in embryos from *MTD-Gal4>>UAS-shRNA-hb* females (B6). The vertical lines show the posterior boundary of the anterior expression domain and both boundaries of the posterior domain for each class. The posterior expression domain is unchanged in the *hb* RNAi embryos, while the anterior pattern shifts anteriorly by 10% egg length. Error bars indicate standard deviations. For WT n = 11, for *hb* RNAi n = 9.

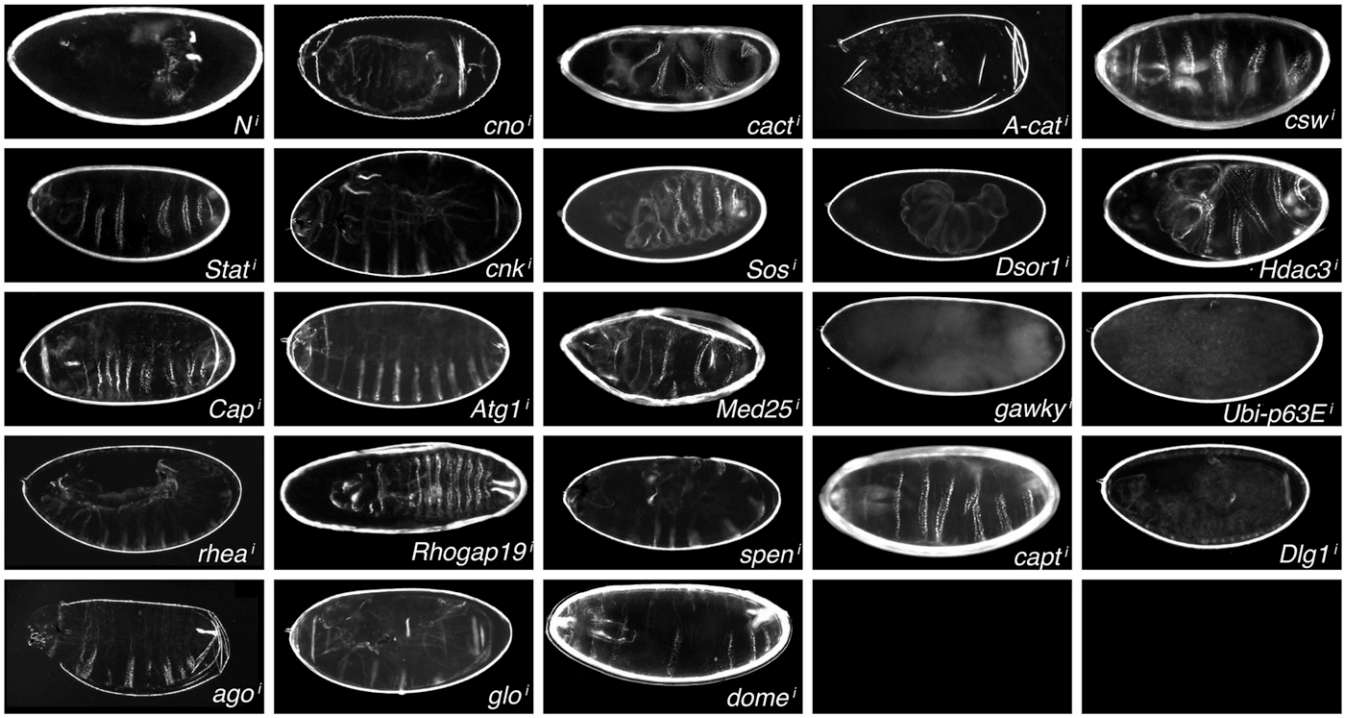

Figure 5 Embryonic phenotypes associated with Mat&Zyg genes. F_2 embryonic phenotypes of embryos derived from *maternal-Gal4>>UAS-shRNA* females crossed to *UAS-shRNA* males. Details on the shRNA lines associated with F_2 phenotypes can be found in Table 1 and the text.

hunchback depletion illustrates the temporal efficacy of Mat-Gal4–mediated RNAi

Analysis of the Mat&Zyg gene *hb* provided another example of how shRNA depletion of different pools of mRNAs allows the visualization of distinct embryonic phenotypic classes. Maternally deposited *hb* mRNA is selectively translated in the anterior and degraded in posterior regions, while zygotic *hb* is expressed in an anterior domain and a posterior stripe. Embryos lacking both zygotic and maternal *hb* exhibit a more severe phenotype than zygotic mutant embryos, but maternal *hb* is dispensable, as embryos derived from a *hb* homozygous germline can be rescued by a single paternal copy (Lehmann and Nüsslein-Volhard 1987). Strikingly, embryos derived from *MTD-Gal4>>UAS-shRNA-hb* females exhibit an unusual embryonic lethal phenotype where all the abdominal segments form properly, but two thoracic segments are missing (Figure 4, B1 and B2). This phenotype strongly resembles that of embryos that lack maternal *hb* and have reduced zygotic *hb* (Simpson-Brose *et al.* 1994). This phenotype is similar across embryos with zero, one, or two copies of the *UAS-shRNA-hb* transgene, indicating that zygotically expressed shRNAs do not contribute to this phenotype (see legend Figure 4).

To examine the distribution of *hb* mRNA after knockdown, we stained for *hb* mRNA by *in situ* hybridization. Compared to WT, the position of the posterior stripe is unchanged in embryos derived from *MTD-Gal4>>UAS-shRNA-hb* females (Figure 4, B5 and B6). In contrast, the anterior expression pattern shifts anteriorly by 10% egg length (EL), and in these embryos, *eve* and *ftz* are each expressed in six stripes rather than their normal seven (data not shown). This defect is consistent with the proposed role of maternal *hb* in working with *bcd* to activate zygotic *hb* robustly and precisely (Porcher *et al.* 2010).

The observation that embryos derived from *MTD-Gal4>>UAS-shRNA-hb* have a stronger phenotype than those from *hb* germline chimeras (Lehmann and Nüsslein-Volhard 1987) suggests that some of the maternally loaded shRNAs persisted long enough to knockdown some zygotic *hb* transcripts. Consistent with this model, crossing *MTD-Gal4>>UAS-shRNA-hb* females to *hb/+* males created a second, more severe phenotypic class missing many head structures, as well as the T2, T3, and A1 segments (Figure 4, B3 and B4). This second class resembles embryos that have substantially reduced zygotic expression of anterior *hb* (Wimmer *et al.* 2000). Together with the data from *dpp* and the heterozygous mutants, these results suggest that the poor knockdown of early zygotic genes stems from our inability to deliver enough shRNAs at the appropriate time.

A genetic screen for new Mat&Zyg genes

To date, only ~10% of the genes in *D. melanogaster* have been examined for their maternal functions through the production of GLCs (Perrimon *et al.* 1989, 1996). To demonstrate the efficacy of the maternal-Gal4–shRNA method to characterize the maternal effect of zygotic lethal mutations, we screened >1000 shRNA lines available at the TRiP in either the VALIUM20 or VALIUM22 vector (see *Materials*

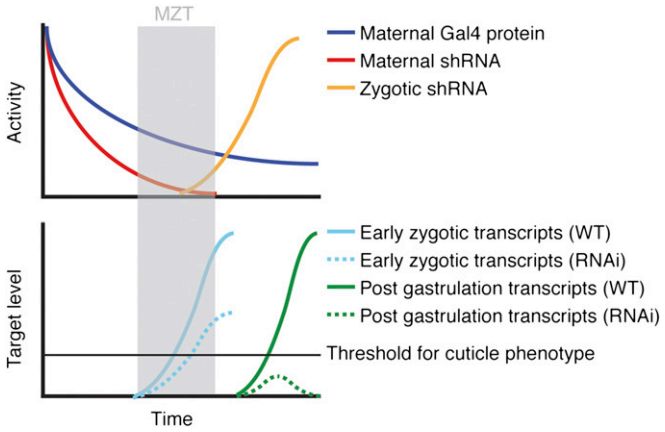

Figure 6 Model for gene knockdown using the "maternal-Gal4–shRNA" system. Maternally deposited shRNAs can deplete early zygotic transcripts only modestly, in most cases not enough to reveal a phenotype (red acting on cyan). Zygotically activated shRNAs can effectively deplete target transcripts when they are expressed before the target is activated (orange acting on green). Early patterning genes escape knockdown because maternally loaded shRNAs lose efficacy over time, and zygotically expressed shRNAs are activated too late. Maternal–zygotic transition (MZT).

and Methods and the TRiP website at www.flyrnai.org) and systematically characterized their F_1 and F_2 phenotypes (Figures 3 and 5 and Table 1). A number of shRNAs targeting known genes illustrate the specificity and efficacy of the shRNA lines. These include *domeless*, *shotgun*, *myospheroid*, (Figure 4), *canoe*, *cactus*, *α-Catenin*, *corkscrew*, and *Stat92E*, *connector enhancer of ksr*, *Son of sevenless*, *discs large 1*, and *Downstream of raf1* (Figure 5). In addition, we recovered novel phenotypes for many genes, in particular the ventralized phenotype associated with *Histone deacetylase 3* (Figure 5), the segment polarity phenotypes of *α-Catenin* (Figure 5), the morphogenesis defects associated with *upheld* (Figure 4) and *split ends* (Figure 5), and the segmentation defects of *archipelago* (Figure 5). Additional information on the screened lines is available at www.flyrnai.org/RSVP. Although further analyses, such as the test of additional independent *UAS-shRNA* lines against the same gene or rescue experiments, will need to be done to confirm that these phenotypes are associated with a knockdown of the intended gene, we note that when we observe a phenotype with an *UAS-shRNA* line against a known gene, it matches with the known loss of function phenotype. This agreement most likely reflects the fact that few genes have very specific mutant cuticle phenotypes, reducing the chance that a phenotype is caused by an off target effect.

Concluding Remarks

We evaluated the efficacy of the Gal4-UAS system to drive shRNA expression in early embryos by performing a number of tests using shRNAs targeting Mat, Zyg, and Mat&Zyg expressed genes. We show that Gal4-driven shRNAs in the female germline efficiently generate mutant phenotypes. In addition, loading the embryo with shRNAs against early zygotic genes was effective in only a few cases (*dpp* and *hb*), possibly because shRNAs are unstable (see model in Figure 6). However, the efficacy of additional shRNAs was unmasked by generating heterozygous mutant zygotic backgrounds. To increase the stability of our shRNAs, we generated two new delivery backbones, which, although effective, did not increase the severity of phenotypes recovered. Interestingly, maternally loaded Gal4 protein, in combination with different copy numbers and delivery methods of *UAS-shRNAs*, can be used to knock down zygotic transcripts in certain time windows and reveal distinct and discrete phenotypes of pleiotropic genes. The system appears especially effective at depleting genes required during mid-embryogenesis after gastrulation (4–5 hr after egg laying). A possible way to improve the efficacy of RNAi in embryos would be to cross *maternal-Gal4>>UAS-shRNA* females to males carrying a strong uniformly expressed zygotic Gal4 driver.

The maternal-Gal4–shRNA method will allow a number of investigations in *Drosophila* embryos. In particular, the opportunity to collect large pools of homogenous embryos will enable biochemical analyses (R. Sopko and N. Perrimon, unpublished results). Further, the technique will be useful for the analysis of regulatory network architecture and *cis*-regulatory element reporter constructs.

Acknowledgments

We are thankful to the Transgenic RNAi Resource Project for providing the shRNA lines used in this study and Lynn Cooley, Daniel St. Johnston, and Fredrick Wirtz-Peitz for the maternal Gal4 driver lines. We acknowledge Richelle Sopko and Rich Binari for helpful discussions, Ben Vincent and Clarissa Scholes for close reading of the manuscript, and Tara Lydiard-Martin for help analyzing the *hb* expression patterns. M.S. was supported by the Harvard Herchel Smith and Harvard Merit fellowships. This work was supported in part by National Institutes of Health GM084947 (N.P). N.P is an investigator of the Howard Hughes Medical Institute.

Literature Cited

Ambrosio, L., A. Mahowald, and N. Perrimon, 1989 Requirement of the Drosophila raf homologue for torso function. Nature 342: 288–291.

Brunner, D., N Oellers, J Szabad, W. HW.H., I I I Biggs, and E. Hafen, 1994 A gain-of-function mutation in Drosophila MAP kinase activates multiple receptor tyrosine kinase signaling pathways. Cell 76: 875–888.

Chou, T., and N. Perrimon, 1996 The autosomal FLP-DFS technique for generating germline mosaics in Drosophila melanogaster. Genetics 144: 1673–1679.

Duffy, J., and N. Perrimon, 1994 The torso pathway in Drosophila: lessons on receptor tyrosine kinase signaling and pattern formation. Dev. Biol. 166: 380–395.

Fowlkes, C., C. L. Luengo Hendriks, S. Keränen, G. Weber, O. Rübel *et al.*, 2008 A quantitative spatiotemporal atlas of gene expression in the Drosophila blastoderm. Cell 133: 364–374.

Fowlkes, C., K. Eckenrode, M. Bragdon, M. Meyer, Z. Wunderlich *et al.*, 2011 A conserved developmental patterning network produces quantitatively different output in multiple species of Drosophila. PLoS Genet. 7: e1002346.

Irish, V., and W. Gelbart, 1987 The decapentaplegic gene is required for dorsal-ventral patterning of the Drosophila embryo. Genes Dev. 1: 868–879.

Kozomara, A., and S. Griffiths-Jones, 2011 miRBase: integrating microRNA annotation and deep-sequencing data. Nucleic Acids Res. 39: D152–D157.

Lawrence, P. A., 1992 *The Making of a Fly: the Genetics of Animal Design*, Blackwell Scientific Publications, Oxford, UK.

Lehmann, R., and C. Nüsslein-Volhard, 1987 hunchback, a gene required for segmentation of an anterior and posterior region of the Drosophila embryo. Dev. Biol. 119: 402.

Lehmann, R., U. Dietrich, F. Jimenez, and J. A. Campos-Ortega, 1981 Mutations of early neurogenesis in Drosophila. Dev. Genes Evol. 190: 226–229.

Li, W., 2005 Functions and mechanisms of receptor tyrosine kinase Torso signaling: lessons from Drosophila embryonic terminal development. Dev. Dyn. 232: 656–672.

Luengo Hendriks, C. L., S. Keranen, C. Fowlkes, L. Simirenko, G. Weber *et al.*, 2006 Three-dimensional morphology and gene expression in the Drosophila blastoderm at cellular resolution I: data acquisition pipeline. Genome Biol. 7: R123.

Ni, J., R. Zhou, B. Czech, L. Liu, L. Holderbaum *et al.*, 2011 A genome-scale shRNA resource for transgenic RNAi in Drosophila. Nat. Methods 8: 405–407.

Peifer, M., C. Rauskolb, M. Williams, B. Riggleman, and E. Wieschaus, 1991 The segment polarity gene armadillo interacts with the wingless signaling pathway in both embryonic and adult pattern formation. Development 111: 1029–1043.

Perrimon, N., L. Engstrom, and A. P. Mahowald, 1985 A pupal lethal mutation with a paternally influenced maternal effect on embryonic development in Drosophila melanogaster. Dev. Biol. 110: 480–491.

Perrimon, N., L. Engstrom, and A. Mahowald, 1989 Zygotic lethals with specific maternal effect phenotypes in Drosophila melanogaster. I. Loci on the X chromosome. Genetics 121: 333–352.

Perrimon, N., A. Lanjuin, C. Arnold, and E. Noll, 1996 Zygotic lethal mutations with maternal effect phenotypes in Drosophila melanogaster. II. Loci on the second and third chromosomes identified by P-element-induced mutations. Genetics 144: 1681–1692.

Petrella, L., T. Smith-Leiker, and L. Cooley, 2007 The Ovhts polyprotein is cleaved to produce fusome and ring canal proteins required for Drosophila oogenesis. Development 134: 703–712.

Porcher, A., A. Abu-Arish, S. Huart, B. Roelens, C. Fradin *et al.*, 2010 The time to measure positional information: maternal hunchback is required for the synchrony of the Bicoid transcriptional response at the onset of zygotic transcription. Development 137: 2795–2804.

Ruby, J., A. Stark, W. Johnston, M. Kellis, D. Bartel *et al.*, 2007 Evolution, biogenesis, expression, and target predictions of a substantially expanded set of Drosophila microRNAs. Genome Res. 17: 1850–1864.

Simpson-Brose, M., J. Treisman, and C. Desplan, 1994 Synergy between the hunchback and bicoid morphogens is required for anterior patterning in Drosophila. Cell 78: 855–865.

Spencer, F. A., F. M. Hoffmann, and W. M. Gelbart, 1982 Decapentaplegic: a gene complex affecting morphogenesis in Drosophila melanogaster. Cell 28: 451–461.

St. Johnston, D., and C. Nusslein-Volhard, 1992 The origin of pattern and polarity in the Drosophila embryo. Cell 68: 201–219.

Tadros, W., and H. Lipshitz, 2009 The maternal-to-zygotic transition: a play in two acts. Development 136: 3033–3042.

Votruba, S. M., 2009 miRNAs in the *Drosophila* egg and early embryo. Master's Thesis, University of Toronto.

Wimmer, E., A. Carleton, P. Harjes, T. Turner, and C. Desplan, 2000 Bicoid-independent formation of thoracic segments in Drosophila. Science 287: 2476–2479.

Communicating editor: T. Schupbach

GENETICS

Supporting Information
http://www.genetics.org/lookup/suppl/doi:10.1534/genetics.112.144915/-/DC1

Depleting Gene Activities in Early *Drosophila* Embryos with the "Maternal-Gal4–shRNA" System

Max V. Staller, Dong Yan, Sakara Randklev, Meghan D. Bragdon, Zeba B. Wunderlich, Rong Tao, Lizabeth A. Perkins, Angela H. DePace, and Norbert Perrimon

DOI: 10.1534/genetics.112.144915

Table S1 List of oligos for cloning shRNAs in miRNA backbones. Complementary oligos were annealed and cloned into VALIUM20 as described in the methods.

mir-275 backbone		
Gene Name	**Top Oligo**	**Bottom Oligo**
ovarian tumor (otu)	ctagctgtaaagtctcctaccttgGCAGAACAACACTGATCAACActggtttttttatatacagTGTTGATCAGTGTTGTTCTGCcgtggtggcagacatatatg	aattcatatatgtctgccaccacgGCAGAACAACACTGATCAACActgtatataaaaaaaccagTGTTGATCAGTGTTGTTCTGCcaaggtaggagactttacag
bicoid (bcd)	ctagctgtaaagtctcctaccttgAACGGGAGCGATAAACTACAActggtttttttatatacagTTGTAGTTTATCGCTCCCGTTcgtggtggcagacatatatg	aattcatatatgtctgccaccacgAACGGGAGCGATAAACTACAActgtatataaaaaaaccagTTGTAGTTTATCGCTCCCGTTcaaggtaggagactttacag
giant (gt)	ctagctgtaaagtctcctaccttgCAGCTAGCTATTAATGTTTAActggtttttttatatacagTTAAACATTAATAGCTAGCTGcgtggtggcagacatatatg	aattcatatatgtctgccaccacgCAGCTAGCTATTAATGTTTAActgtatataaaaaaaccagTTAAACATTAATAGCTAGCTGcaaggtaggagactttacag

miR-92a backbone		
Gene Name	**Top Oligo**	**Bottom Oligo**
Notch (N)	ctagcaatatgaatttcccgGCGGCGGTTAACAATACCGAAAttttgcatttcgaataaaTTCGGTATTGTTAACCGCCGCtgggcggtttgtaataaacag	aattctgtttattacaaaccgcccaGCGGCGGTTAACAATACCGAAtttattcgaaatgcaaaaTTCGGTATTGTTAACCGCCGCcgggaaattcatattg
bicoid (bcd)	ctagcaatatgaatttcccgAACGGGAGCGATAAACTACAAttttgcatttcgaataaaTTGTAGTTTATCGCTCCCGTTtgggcggtttgtaataaacag	aattctgtttattacaaaccgcccaAACGGGAGCGATAAACTACAAtttattcgaaatgcaaaaTTGTAGTTTATCGCTCCCGTTcgggaaattcatattg
Kruppel (Kr)	ctagcaatatgaatttcccgTTGTTGCTGCTTCAAATATAAttttgcatttcgaataaaTTATATTTGAAGCAGCAACAAtgggcggtttgtaataaacag	aattctgtttattacaaaccgcccaTTGTTGCTGCTTCAAATATAAttattcgaaatgcaaaaTTATATTTGAAGCAGCAACAAcgggaaattcatattg
wingless (wg)	ctagcaatatgaatttcccgACGAATAGATTTCAAGAAGAAAttttgcatttcgaataaaTTCTTCTTGAAATCTATTCGTtgggcggttgtaataaacag	aattctgtttattacaaaccgcccaACGAATAGATTTCAAGAAGAAtttattcgaaatgcaaaaTTCTTCTTGAAATCTATTCGTcgggaaattcatattg
armadillo (arm)	ctagcaatatgaatttcccgTACGATTGCTGTTCAACGAAAtttttgcatttcgaataaaTTTCGTTGAACAGCAATCGTAtgggcggtttgtaataaacag	aattctgtttattacaaaccgcccaTACGATTGCTGTTCAACGAAAtttattcgaaatgcaaaaTTTCGTTGAACAGCAATCGTAcgggaaattcatattg